Journal of Intelligent and Robotic Systems **14**: 21–41, 1995.

The Mechanical Design of a Seven-Axes Manipulator with Kinematic Isotropy

F. RANJBARAN, J. ANGELES and M. A. GONZÁLEZ-PALACIOS
Department of Mechanical Engineering and McGill Centre for Intelligent Machines
McGill University, 817 Sherbrooke St., West Montreal, Canada H3A 2K6

and

R. V. PATEL
Department of Electrical and Computer Enginnering, Concordia University
1455 De Maisonneuve Blvd., West Montreal, Canada, H3G 1M8

(Received: 28 December 1993)

Abstract. Discussed in this paper are the issues underlying the mechanical design of a seven-axes isotropic manipulator. The kinematic design of this manipulator was made based on one main criterion, namely, accuracy. Thus, the main issue determining the underlying architecture, defined by its Hartenberg–Denavit (HD) parameters, was the optimization of its kinematic conditioning. This main criterion led not to one set of HD parameters, but rather to a manifold of these sets, which allowed the incorporation of further requirements, such as structural behavior, workspace considerations and functionality properties. These requirements in turn allowed the determination of the link shapes and the selection of actuators. The detailed mechanical design led to heuristic rules that helped in the decision-making process in defining issues such as link sub-assemblies and motor location along the joint axes.

Key words. Design, heuristic rules, kinematic isotropy, manipulator, redundant.

1. Introduction

In this paper we present an overview of the design and manufacturing of a redundant seven-axes manipulator with an isotropic architecture for six-dimensional Cartesian tasks. This manipulator is henceforth referred to as REDIESTRO (RE-Dundant, Isotropically Enhanced, Seven-Turning-pair RObot) for brevity. In the design of conventional serial-type manipulators only a few simplifying kinematic criteria have been considered. For nonredundant manipulators, the kinematic design has been mainly oriented towards achieving *kinematic solvability* and *manufacturing feasibility*. These criteria, in turn, have led to the existence of a particular class of manipulators whose axes are either parallel or perpendicular, i.e., orthogonal manipulators. Here, we mean by orthogonal a manipulator whose

consecutive axes make angles that are multiples of 90°; for example, manipulators with spherical wrists [1], or with planar two-revolute subchains. Moreover, a general classification of manipulators with simple inverse kinematics is reported in [2]. The associated simple inverse kinematics has been formulated by exploiting the special features, like orthogonality, of the kinematic structures of these robots. With the advent of fast and general inverse kinematics algorithms developed in the last ten years, however, the need of simple kinematic structures is less dominant. On the other hand, parallelism and orthogonality of the axes can give rise to undesirable singularities. These singularities are manifested, for example in the rate control and kinematic calibration of these manipulators [3, 4]. Serving the two foregoing objectives excludes a major class of manipulators with general architectures. By exploring general manipulator architectures, one can not only improve the numerical conditioning of the manipulator kinetostatic maps, but also take into consideration other critical issues pertinent to the design and realization of the overall robotic system.

For the case of redundant manipulators, general design criteria have been proposed. For example, Hollerbach [5] outlined the following features as guidelines for the design of these manipulators:

- Elimination of internal singularities;
- Optimization of workspace;
- Kinematic simplicity;
- Mechanical constructability.

It is evident that the foregoing criteria highlight critical issues for the design of *general* redundant manipulators. Recently, some researchers have emphasized methodologies for the design of redundant manipulators for specific tasks or classes of tasks. In this regard, the framework of *task-based design* for *reconfigurable modular manipulators* has been introduced [6–9]. In the design process of REDIESTRO we have been mainly concerned with its kinetostatic accuracy. Thus, the main issue determining the architecture of REDIESTRO, defined by its Hartenberg–Denavit (HD) parameters [10], was the optimization of its kinematic conditioning. This main criterion led not to one set of HD parameters, but rather to a manifold of these sets, which allowed the incorporation of further requirements. In addition to the design criteria listed above, we have considered issues such as maximum reach, structural behavior, link-motor collision consideration, and functionality properties. These requirements, in turn, allowed the determination of the link shapes and the selection of actuators. It has to be noted that REDIESTRO is not designed for any particular task or family of tasks, but rather to show the merits of kinematic isotropy as a main criterion in manipulator design, and to compare the enhanced accuracy with respect to non-isotropic

manipulators. In the sections below, we will discuss the overall strategy based on the integration of different aspects and stages of the design process and will discuss our heuristic rules.

2. Design Methodology

The major design activities undertaken from the start of the project to the preparation of the shop drawings of REDIESTRO are listed below:

1. Kinematic design;
2. Preliminary mechanical design;
3. Detailed mechanical design;
4. Three-dimensional rendering and animation; and
5. Redundancy resolution and kinematic simulation.

The first four items will be discussed in detail presently, while the last item will be addressed in a later paper. The activities mentioned above have been integrated into a hierarchical framework that consists of three different iterative loops at different levels. The flow diagram shown In Figure 1 depicts these activities and the corresponding loops.

The inner loop of the top half of Figure 1 consists of the *kinematic design* and *skeleton rendering* of the resulting architectures. Numerical optimization techniques were utilized for the kinematic design, whereby a set of different isotropic seven-axes manipulators was obtained. Three-dimensional visualization of the corresponding models in the form of simple skeleton renderings were then analyzed for functionality and load-carrying requirements, and additional structural requirements were imposed to narrow even more the selection set. As a result of this loop, a first candidate was chosen and the corresponding normalized HD parameters were identified.

The second loop includes the *kinematic* and *preliminary mechanical design*. At this stage the candidate manipulator was scaled, based on the requirements on the volume of the workspace and maximum reach. A preliminary mechanical analysis based on required performance characteristics of the manipulator was then performed and the actuators were selected. Furthermore, a preliminary layout of the links and placement of the actuators were also proposed. Functionality issues of the design and actuator placements required further constraints on the HD parameters. This demand was achieved by imposing additional constraints on the kinematic optimization schemes whereby the final scaled HD parameters were determined.

The final design loop consists of the *detailed mechanical design, detailed three-dimensional renderings* and animation. In this loop, with the given HD

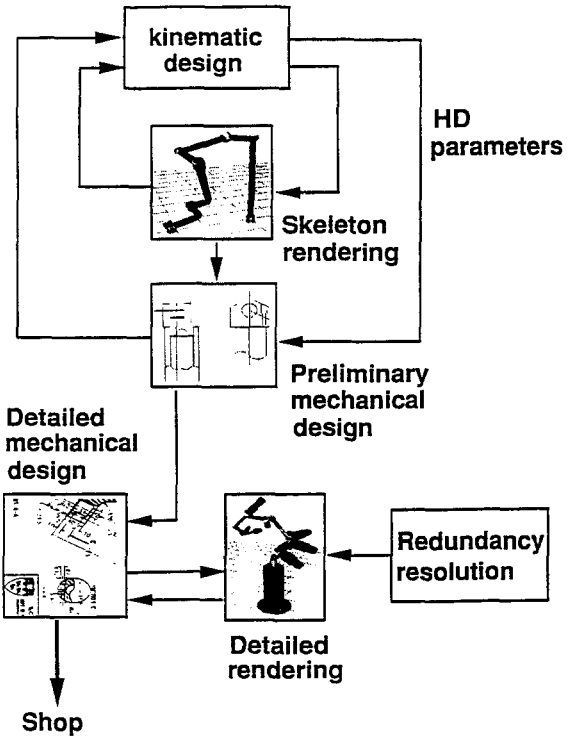

Fig. 1. Flow diagram of the design methodology.

parameter and actuator specifications, the detailed mechanical design of the links was performed. Issues such as workspace requirements, range of motion of each joint and collision of the link-actuator sub-assemblies were set forth as final design requirements. These issues were analyzed using detailed three-dimensional renderings of the assembled manipulator and thus, the required modifications on the shape and geometry of the link sub-assemblies were made. In the sections below, each major part of the design process mentioned above will be discussed in more detail.

3. Kinematic Design

The approach taken for the kinematic design of REDIESTRO is based on previous work by Angeles *et al.* [11]. Here we give a short account on the Jacobian matrix and its central role in the kinematic analysis and synthesis of serial-type manipulators. In analysis, information that can be inferred from the Jacobian matrix **J** comprises issues such as kinetostatic conditioning and singularities of the joint rate and torque mappings [12–16], kinematic calibration [4], workspace volume quantization [17] and maximum reach. Moreover, entries of the Jacobian matrix can be used in manipulator synthesis, as pointed out by González-Palacios

et al. [18]. Thus, the Jacobian matrix can be suitably chosen as a crucial element in manipulator design.

By adopting the HD parameters, the manipulator architecture can be represented schematically as shown in Figure 2. Links are numbered $0, 1, \ldots, n$, and the ith pair is defined as that coupling the $(i-1)$st with the ith link, with link 0 being the fixed base. The end-effector is attached to the last link whose operation point is denoted by P. Next, a coordinate frame is defined with origin O_i and axes X_i, Y_i, Z_i which is attached to the $(i-1)$st link, for $i = 1, \ldots, n+1$. Furthermore, Z_i is the axis of the ith pair, X_i is defined as the common perpendicular to Z_{i-1} and Z_i, directed from the former to the latter. Moreover, the *distance* between Z_i and Z_{i+1} is defined as a_i, which is, thus, *nonnegative*. The Z_i-coordinate of the intersection O_i' of Z_i with X_{i+1} is denoted by b_i, whose absolute value is the distance between X_i and X_{i+1}. The *twist angle* α_i, is the angle between Z_i and Z_{i+1} and is measured about the positive direction of X_{i+1}. Finally, θ_i is the angle between X_i and X_{i+1} and is measured about the positive direction of Z_i.

The Jacobian matrix of a general n-revolute joint manipulator takes the form [19]

$$\mathbf{J} = \begin{bmatrix} \mathbf{e}_1 & \mathbf{e}_2 & \cdots & \mathbf{e}_n \\ \mathbf{e}_1 \times \mathbf{r}_1 & \mathbf{e}_2 \times \mathbf{r}_2 & \cdots & \mathbf{e}_n \times \mathbf{r}_n \end{bmatrix}, \tag{1}$$

where $\mathbf{e}_i$ is the unit vector parallel to the axis of the ith revolute joint and $\mathbf{r}_i$ is the vector directed from any point on the same axis to the operation point P of the end-effector, as shown in Figure 2. Furthermore, the ith column of $\mathbf{J}$ comprises the *normalized Plücker coordinates* of the ith axis of the manipulator [20].

The numerical conditioning of the Jacobian matrix plays a crucial role when investigating the kinetostatic performance of a manipulator. Specifically, when

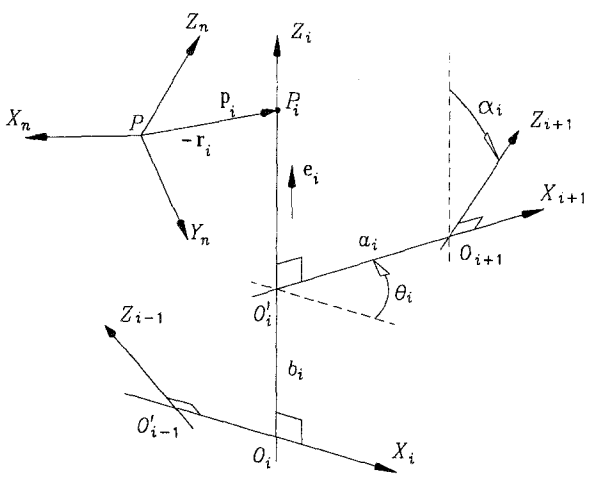

Fig. 2. The basic notation.

relating the joint-rate vector $\dot{\theta}$ with the twist vector $\mathbf{t}$ of the end-effector, or the joint torque vector τ with the wrench $\mathbf{w}$, applied at the operation point, we have

$$\mathbf{J}\dot{\theta} = \mathbf{t}, \tag{2a}$$

$$\mathbf{J}^T\mathbf{w} = \tau, \tag{2b}$$

where $\mathbf{t}$ and $\mathbf{w}$ are defined as six-dimensional vectors, namely,

$$\mathbf{t} \equiv \begin{bmatrix} \omega \\ \dot{\mathbf{p}} \end{bmatrix} \quad \text{and} \quad \mathbf{w} \equiv \begin{bmatrix} \mathbf{n} \\ \mathbf{f} \end{bmatrix},$$

with ω and $\dot{\mathbf{p}}$ defined, respectively, as the angular velocity of the end-effector and the velocity of the operation point P, while $\mathbf{n}$ and $\mathbf{f}$ denote the moment applied at the end-effector and the force acting at point P, respectively. If in Equations (2a) and (2b) $\mathbf{J}$ has a large condition number, small perturbations in the data, i.e. in the entries of $\mathbf{J}$ and the components of $\mathbf{t}$ and $\mathbf{w}$, may cause large changes in the computed values of $\dot{\theta}$ and τ. Matrices with condition numbers above a certain allowable bound are termed *ill-conditioned* because of this undesired behaviour. Optimally-conditioned matrices, on the other hand, are those with a condition number of unity, and are called *isotropic*. The worst-conditioned are singular matrices, with a condition number of infinity.

A measure of the numerical conditioning of matrices is the condition number κ [21] that, for any matrix $\mathbf{A}$ can be defined as

$$\kappa(\mathbf{A}) \equiv \|\mathbf{A}\| \, \|\mathbf{A}^{-1}\| \tag{3}$$

where $\|\cdot\|$ denotes any norm of its matrix argument. By adopting the 2-norm for matrices, the foregoing definition takes on the form

$$\kappa(\mathbf{A}) = \frac{\sigma_{\max}}{\sigma_{\min}} = \sqrt{\frac{\lambda_{\max}}{\lambda_{\min}}}$$

where $\sigma_{\max}$ and $\sigma_{\min}$ are, respectively, the maximum and minimum singular values of $\mathbf{A}$, while $\lambda_{\max}$ and $\lambda_{\min}$ are the largest and smallest eigenvalues of $\mathbf{A}\mathbf{A}^T$. This definition of the condition number based on the singular values of a matrix can be applied to both square and rectangular matrices. For instance, if $\mathbf{A}$ is an $m \times n$ matrix, with $m < n$, then the singular values of $\mathbf{A}$ are the nonnegative square roots of the eigenvalues of the $m \times m$ symmetric positive-semidefinite matrix $\mathbf{A}\mathbf{A}^T$. Next, the condition number of $\mathbf{A}$ is defined as the square root of the ratio of the largest to the smallest eigenvalues of $\mathbf{A}\mathbf{A}^T$. Hence, a matrix is isotropic if all its singular values are identical and nonzero. This is equivalent to saying that, if $\mathbf{A}$ is isotropic, then a real number σ exists such that

$$\mathbf{A}\mathbf{A}^T = \sigma^2\mathbf{1}_m \tag{4}$$

where σ is the common singular value of $\mathbf{A}$, and $\mathbf{1}_m$ is the $m \times m$ identity matrix. As discussed by Li [22], the condition number of the Jacobian matrix is frame-invariant, but depends on the location of the operation point of the end-effector. However, Angeles *et al.* [11], pointed out that this dependency is, in fact, favorable when investigating manipulator dexterity, for it allows us to distinguish between the performances of two different end-effectors, even if attached to the same manipulator with different operation points.

The concept of kinematic isotropy was first introduced by Salisbury and Craig [23], for the optimum design of mechanical fingers. An extension of isotropy to other manipulators is given in [14], where the conditioning index of manipulators based on the condition number of the Jacobian matrix is introduced, and thus, a manipulator is called isotropic if it can attain a set of configurations in its workspace at which the underlying Jacobian matrix is isotropic. The kinematic design of general isotropic manipulators has been presented in [16], [24], and [11], based on isotropic Jacobian matrices. Kinematic isotropy has also been extended to the design of automatic guided vehicles (AGVs) and systems with time varying topologies, such as walking machines and multifingered hands [25, 26].

From Equation (1) it is apparent that the columns of $\mathbf{J}$ are not dimensionally homogeneous, as the unit vectors $\mathbf{e}_i$ are dimensionless, while vectors $\mathbf{e}_i \times \mathbf{r}_i$ have units of length. This dimensional inhomogeneity gives rise to inconsistencies when evaluating the condition number under discussion, for it prevents us from ordering the singular values of the Jacobian matrix from smallest to largest. We circumvent this problem by performing a normalization of the entries of the Jacobian matrix, by dividing the last three rows of $\mathbf{J}$ by a *characteristic length* L, thereby providing a dimensionally homogeneous Jacobian matrix that we denote by $\bar{\mathbf{J}}$, namely,

$$\mathbf{J} = \begin{bmatrix} \mathbf{e}_1 & \mathbf{e}_2 & \cdots & \mathbf{e}_n \\ \frac{1}{L}\mathbf{e}_1 \times \mathbf{r}_1 & \frac{1}{L}\mathbf{e}_2 \times \mathbf{r}_2 & \cdots & \frac{1}{L}\mathbf{e}_n \times \mathbf{r}_n \end{bmatrix}. \tag{5}$$

We can now rewrite the isotropy condition (4) for the normalized Jacobian matrix as

$$\bar{\mathbf{J}}\bar{\mathbf{J}}^T = \begin{bmatrix} \sum_1^n \mathbf{e}_k \mathbf{e}_k^T & \frac{1}{L}\sum_1^n \mathbf{e}_k (\mathbf{e}_k \times \mathbf{r}_k)^T \\ \frac{1}{L}\sum_1^n \mathbf{e}_k (\mathbf{e}_k \times \mathbf{r}_k)^T & \frac{1}{L}\sum_1^n (\mathbf{e}_k \times \mathbf{r}_k)(\mathbf{e}_k \times \mathbf{r}_k)^T \end{bmatrix} = \sigma^2 \mathbf{1}_6. \tag{6}$$

If $\bar{\mathbf{J}}$ is made isotropic, then the upper-left block of the foregoing matrix equation yields

$$\sum_1^n \mathbf{e}_k \mathbf{e}_k^T = \sigma^2 \mathbf{1}_3.$$

Upon equating the trace of both sides of the above equation, we obtain

$$n = 3\sigma^2$$

where $\text{tr}\left[\sum_1^n \mathbf{e}_k \mathbf{e}_k^T\right] \equiv \sum_1^n \mathbf{e}_k^T \mathbf{e}_k$ and hence,

$$\sigma = \sqrt{\frac{n}{3}}. \tag{7}$$

Furthermore, using the lower-right block in Equation (6), we can uniquely solve for L as shown below

$$\text{tr}\left[\frac{1}{L^2}\sum_1^n (\mathbf{e}_k \times \mathbf{r}_k)(\mathbf{e}_k \times \mathbf{r}_k)^T\right] = 3\sigma^2$$

or

$$\frac{1}{L^2}\sum_1^n \|\mathbf{e}_k \times \mathbf{r}_k\|^2 = 3\sigma^2$$

and, substituting for σ from Equation (7) in the foregoing equation, we have

$$L^2 = \frac{\sum_1^n \|\mathbf{e}_k \times \mathbf{r}_k\|^2}{n}. \tag{8}$$

It is interesting to note that the foregoing expression reveals a geometric interpretation of the characteristic length, i.e., L is the root-mean squared (RMS) value of the distances of the n joint axes to the operation point of the end-effector at the isotropic posture of the manipulator. Although this expression for L was derived by making use of the isotropy of $\bar{\mathbf{J}}$, we will show below that it can be used for non-isotropic manipulators as well, upon minimizing the condition number of the associated Jacobian matrix. In order to show this, we will use an estimate of the condition number $\tilde{\kappa}$ based on geometric and algebraic means of the singular values of $\mathbf{J}$ [27],

$$\tilde{\kappa} \equiv \frac{A}{B}, \tag{9}$$

where

$$A \equiv \frac{\text{tr}\left(\bar{\mathbf{J}}\bar{\mathbf{J}}^T\right)}{m} = \frac{\sigma_1^2 + \sigma_2^2 + \cdots + \sigma_m^2}{m}$$

and

$$B \equiv \left(\det \bar{\mathbf{J}}\bar{\mathbf{J}}^T\right)^{1/m} = \left(\sigma_1^2 \sigma_2^2 \cdots \sigma_m^2\right)^{1/m},$$

with σ_i being the ith singular value of $\bar{\mathbf{J}}$ and m being the dimension of the task space (i.e., $m = 6$ for a positioning and orienting manipulator). It is evident that $\tilde{\kappa}$ as defined in this way is, in fact, the ratio of the algebraic to the geometric means of the squares of the singular values of $\bar{\mathbf{J}}$.

For a non-isotropic $\mathbf{J}$ we can rewrite Equation (6) while using a normalizing length $\tilde{L}$, as yet to be determined, namely,

$$\bar{\mathbf{J}}\bar{\mathbf{J}}^T = \begin{bmatrix} \sum_1^n \mathbf{e}_k \mathbf{e}_k^T & \frac{1}{\tilde{L}} \sum_1^n \mathbf{e}_k (\mathbf{e}_k \times \mathbf{r}_k)^T \\ \frac{1}{\tilde{L}} \sum_1^n \mathbf{e}_k (\mathbf{e}_k \times \mathbf{r}_k)^T & \frac{1}{\tilde{L}^2} \sum_1^n (\mathbf{e}_k \times \mathbf{r}_k)(\mathbf{e}_k \times \mathbf{r}_k)^T \end{bmatrix}. \tag{10}$$

Moreover, for $m = 6$ we have

$$\det\left(\bar{\mathbf{J}}\bar{\mathbf{J}}^T\right) = \frac{\det\left(\mathbf{J}\mathbf{J}^T\right)}{\tilde{L}^6} \tag{11}$$

and

$$\operatorname{tr}\left(\bar{\mathbf{J}}\bar{\mathbf{J}}^T\right) \equiv \operatorname{tr}\left(\sum_1^n \mathbf{e}_k \mathbf{e}_k^T\right) + \frac{1}{\tilde{L}^2} \operatorname{tr}\left(\sum_1^n (\mathbf{e}_k \times \mathbf{r}_k)(\mathbf{e}_k \times \mathbf{r}_k)^T\right), \tag{12}$$

$$\operatorname{tr}\left(\bar{\mathbf{J}}\bar{\mathbf{J}}\right)^T = n + \frac{\sum_1^n \|\mathbf{e}_k \times \mathbf{r}_k\|^2}{\tilde{L}^2}. \tag{13}$$

Hence,

$$\tilde{\kappa}^2 = \frac{6n\tilde{L}^2 + \sum_1^n \|\mathbf{e}_k \times \mathbf{r}_k\|^2}{6\tilde{L}\left[\det\left(\mathbf{J}\mathbf{J}^T\right)\right]^{1/6}}. \tag{14}$$

Next, in order to find $\tilde{L}$ so as to minimize $\tilde{\kappa}$ we set $\partial\tilde{\kappa}^2/\partial\tilde{L}$ equal to zero which yields an equation for $\tilde{L}^2$ as

$$\tilde{L}^2 = \frac{\sum_1^n \|\mathbf{e}_k \times \mathbf{r}_k\|^2}{n}$$

which is the same as the characteristic length L for an isotropic n-axes manipulator for positioning and orienting tasks. This formula for $\tilde{L}$ is configuration-dependent and for non-isotropic manipulators, can be applied at configurations where the Jacobian matrix attains its minimum condition number. The merits of the characteristic length, as defined above, go beyond the realm of dimensional consistency, for, it can be used as a very useful normalizing tool when comparing manipulators for dexterity and workspace volume in the design process.

3.1. ISOTROPIC DESIGN

With regard to the isotropic design of seven-axes manipulators for positioning and orienting tasks, Equation (6) gives rise to 21 independent nonlinear equations. It is required to determine the set of Hartenberg–Denavit parameters [10] (Figure 2), together with the characteristic length of the manipulator that renders the Jacobian matrix isotropic. Hence we aim at making $\bar{\mathbf{J}}\bar{\mathbf{J}}^T$ to approach $\sigma^2\mathbf{1}_6$. To this end we define a symmetric matrix $\mathbf{M}$ as

$$\mathbf{M} \equiv \mathbf{J}\mathbf{J}^T - \sigma^2\mathbf{1}_6 \tag{15}$$

and attempt to zero all 21 independent entries of $\mathbf{M}$. From the total number of 28 HD parameters to be determined, only 25 will affect the condition number, and thus, will be included in the optimization procedure. This is so because variations of the first offset distance and joint angle, b_1 and θ_1, respectively, produce rigid body motions of the overall manipulator, and thus leave the frame-invariant condition number unchanged. Furthermore, the entries of the Jacobian matrix are independent of the last twist angle α_7. We eliminate the three aforementioned variables by pre-setting them equal to zero and, hence, we are left with 25 HD parameters and the characteristic length as our design variables. These variables are then grouped into a 26-dimensional design vector $\mathbf{x}$, to be determined numerically. Furthermore, we denote by $\mathbf{f}$ the 21-dimensional vector function obtained from Equation (15). Hence, we can redefine the design problem as

$$\min_{\mathbf{x}} \|\mathbf{f}(\mathbf{x})\|^2. \tag{16}$$

For a general isotropic design, no constraints are imposed on the foregoing optimization problem. However, a solution for $\mathbf{x}$ may very well include a link length a_i that is negative. Since a_i is defined as a positive quantity that represents the *length* of a link, it seems that we need to add constraints to our optimization formulation to limit the search domain of $\{a_i\}_1^n$ to positive values only. However, instead of doing so, we at first do not impose this constraint to the problem but, if any of the resulting a_i values turns out to be negative, we simply take its absolute value as the corresponding link length by making the simple adjustments of the other parameters that leave the relative position and orientation of the two consecutive joints involved unchanged, namely

if $a_k < 0$, for $k < n$ then,
  $a_k \leftarrow |a_k|$
  $\theta_k \leftarrow \theta_k - \pi$
  $\theta_{k+1} \leftarrow \theta_{k+1} - \pi$
  $\alpha_{k-1} \leftarrow |\alpha_{k-1}|$
endif

and

$$\begin{aligned}
&\text{if } a_n < 0, \qquad \text{then,}\\
&\quad a_n \leftarrow |a_n|\\
&\quad \theta_n \leftarrow \theta_n - \pi\\
&\quad \alpha_{n-1} \leftarrow |\alpha_{n-1}|\\
&\text{endif}
\end{aligned}$$

3.2. NUMERICAL RESULTS

Equation (16) is an underdetermined system of 21 equations, in 26 unknows that, in general, admits an infinite number of solutions. As a first trial, the foregoing equation was solved by using a least-squares approach, implemented on MATLAB^{TM}. The nondimensional results obtained for this design, after making the appropriate adjustments discussed before, are given in Table I, while Figure 3 depicts a three-dimensional skeleton rendering of this manipulator in its isotropic configuration. As discussed earlier, the integration of the optimization and the three-dimensional visualization schemes forms a design loop, from which several other solutions can be obtained and analyzed. At this stage, and based on other design objectives, desired constraints can be imposed on the formulation. For instance, from a structural viewpoint, it would be advantageous if we could concentrate as much mass of the arm as possible over the base of the manipulator. This would enhance the dynamic performance and the structural rigidity of the manipulator. By preassigning values to five of the components of $\mathbf{x}$, namely a_1, a_3, a_5, b_2 and b_4, the optimization problem will then be transformed into solving a determined set of 21 nonlinear equations in 21 unknowns.

Moreover, by using the Newton–Raphson method, the associated set of nonzero HD parameters were obtained using MATLAB's *fsolve* routine. Table II contains

Table I. HD parameters for the fully isotropic configuration.
Design No. 1

Link i	a_i	b_i	α_i (deg)	θ_i (deg)
1	0.1154	0	104.6285	180.0000
2	1.5704	−0.0483	−86.3539	40.1118
3	0.1756	1.0226	60.6524	30.5779
4	1.0499	−0.7054	108.6141	−105.7290
5	0.9094	−0.0104	−110.1435	−69.0636
6	0.0053	−0.0614	−107.3289	146.9810
7	0.4810	0.8844	0	33.5665

Characteristic length = 0.7502.

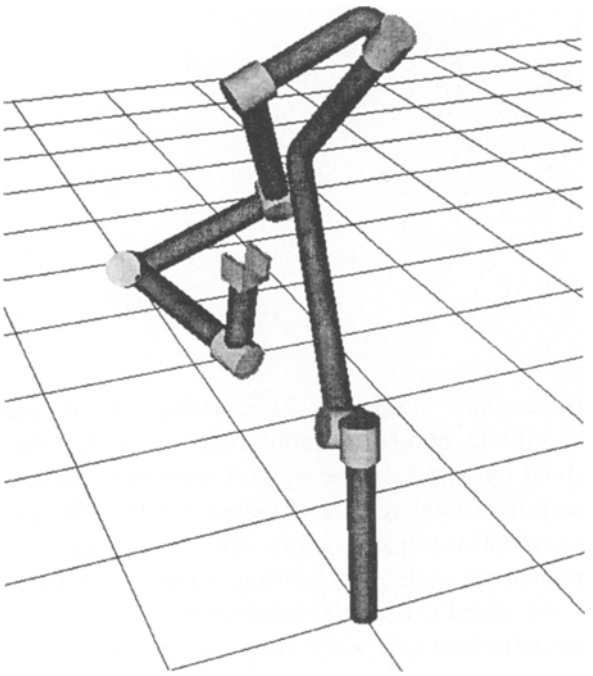

Fig. 3. Isotropic seven-axes manipulator. Design No. 1.

Table II. HD parameters for the candidate manipulator at the isotropic configuration

Link i	a_i	b_i	α_i (deg)	θ_i (deg)
1	0	0	−62.7121	0
2	0.0236	0	−11.0955	35.122
3	0	0.1740	106.6842	62.6876
4	2.2359	0	72.8710	117.7089
5	0	−1.8578	55.8327	−24.6359
6	0.0729	3.2093	62.8430	−2.3153
7	1.1921	−1.4648	0	225.4497
	Characteristic length = 1.0324			

the nondimensional HD parameters for the first candidate manipulator, whose rendering is given in Figure 4.

From Figure 4 it can be observed that, by having the first four joints concentrated very close to the base of the manipulator, the weight of the corresponding links and actuators will be concentrated closer to the base. Having chosen this last solution as the final candidate, the first design loop is completed, and the

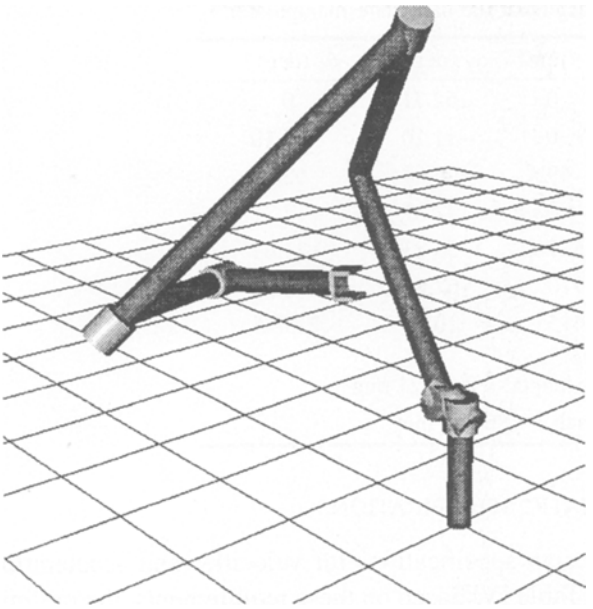

Fig. 4. Isotropic candidate seven-axes manipulator.

procedure is merged with the second loop, which consists of the kinematic and preliminary mechanical designs (Figure 1). At this stage, emphasis is placed on the mechanical design issues that have to be addressed. Moreover, further refinements and minor changes to the HD parameters can still be made by using the numerical technique discussed in the previous section.

4. Preliminary Mechanical Design

At this level, primarily an overall kinematic performance for the manipulator is specified, actuators are selected, and a rudimentary design of the manipulator is performed. Any final minor modifications and/or refinements of the kinematic architecture are made at this stage.

4.1. SCALING OF THE MANIPULATOR

In order to proceed with the design, it is necessary to bring the candidate architecture into its full-scale dimensions. To do this, we require that the manipulator have a reach of 1.0 m when all joint angles are zero. Based on this yardstick we scale the candidate manipulator as given in Table III.

Table III. Scaled parameters of the candidate manipulator

Link i	a_i (mm)	b_i (mm)	α_i (deg)	θ_i (deg)
1	0	0	−62.71	0
2	6.7	0	−11.10	35.10
3	0	49.4	106.68	62.71
4	634.4	0	72.87	117.71
5	0	−527.1	55.83	−24.63
6	20.7	910.6	62.84	−2.32
7	338.2	−415.6	0	225.45
	Characteristic length = 292.921 mm			
	Maximum reach = 1866.05 mm			

4.2. PRELIMINARY KINEMATIC SPECIFICATIONS

The overall preliminary design specifications for velocities and accelerations of different links are given in Table IV. Based on these requirements, the preliminary selection of the actuators is made. For all seven drives, DC servomotors equipped with harmonic drives, incremental encoders and electromagnetic brakes were selected.

Table IV. Design specifications for angular velocities and accelerations

Link axis No.		1	2	3	4	5	6	7
Max. angular velocity	(s^{-1})	1.0	0.8	0.8	0.8	1.65	1.65	1.65
Min. average ang. acc.	(s^{-2})	9.81	7.40	6.94	6.60	11.10	10.38	14.41
Drive output speed	(rpm)	9.55	7.64	7.64	7.65	15.7	15.7	15.7

4.3. PRELIMINARY DESIGN OF THE LINK SUB-ASSEMBLIES

At this stage a rudimentary layout of the link shapes and actuator placement are made, and the conceptual design of the corresponding sub-assemblies is completed. It was observed that, although, keeping the first four of the actuators close to the base is advantageous from the point of view of dynamic performance, installation of the four units at a close vicinity proved to be difficult. In particular, since the joint axes 2 and 3 of the candidate manipulator almost intersect at about 11°, as seen from Table III, and because of the load-carrying capacity of the actuators, the only possible solution was the use of a differential gear train between actuators 2 and 3. A preliminary design of the candidate manipulator with the differential gear train was completed, but is not essential to this discussion and is, hence, omitted.

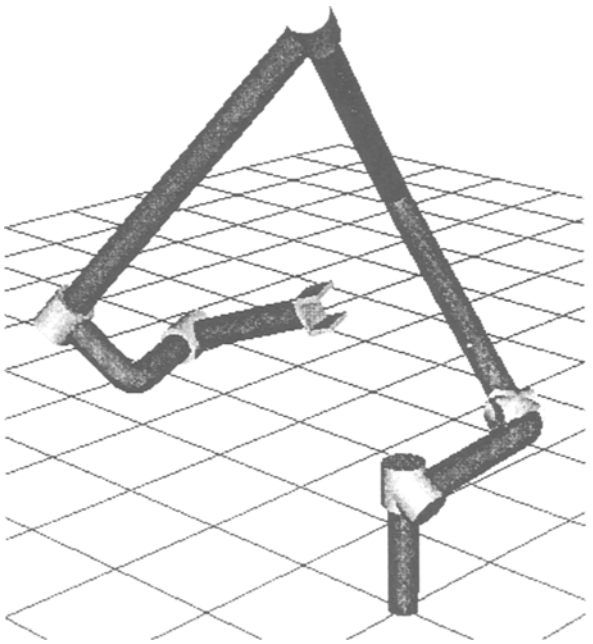

Fig. 5. Skeleton rendering of REDIESTRO at the isotropic configuration.

Table V. Scaled parameters of REDIESTRO

Link i	a_i (mm)	b_i (mm)	α_i (deg)	θ_i (deg)
1	0	0	−58.31	0
2	231.13	−22.91	−20.0289	−11.01
3	0	36.93	105.26	91.94
4	398.84	0	60.91	113.93
5	0	−471.59	59.88	−2.26
6	135.59	578.21	−75.47	150.25
7	334.44	−145.05	0	63.76
	Characteristic length = 220.6505 mm			
	Maximum reach = 1488.0 mm			

Before leaving the last iterative design loop, it was decided that, by modifying the kinematic structure of the manipulator, the differential gear train be eliminated. In order to do this, the link length a_2 was preassigned a minimum value that could enclose two of the selected actuators. In turn, one of the constraints, namely $b_2 = 0$, was relaxed from the numerical formulation of the kinematic design. The outcome of this modification was our final design, whose three-dimensional

skeleton rendering at the isotropic configuration is shown in Figure 5, and whose scaled HD parameters are given in Table V.

It is apparent from Figure 6 and Table V that the first four joints are divided into two separate groups of two joints each, that still lie as close as possible to the base. This completed the iterative kinematic and overall mechanical design loops and, thus, the architecture of REDIESTRO was finalized.

5. Detailed Mechanical Design

Having completed the preliminary kinematic and mechanical designs of REDIESTRO, the detailed mechanical design of the link sub-assemblies was undertaken. The exact shape of each link, together with the location of the corresponding actuators along each joint axis formed the last design loop, as shown in the bottom of the design flow diagram of Figure 1. In this loop, with the aid of RVS, the robotic visualization system developed at the McGill Centre for Intelligent Machines (CIM), a step-by-step design of each link-and-actuator assembly was completed, while monitoring many different issues, such as collisions among links and actuators, feasibility, constructability, minimization of the moment arms as seen by the previous actuator, etc. Figures 6 and 7 are the output of RVS showing REDIESTRO at its zero configuration (i.e., $\theta_i = 0,\ i = 1, \ldots, 7$) and at the maximum reach, respectively.

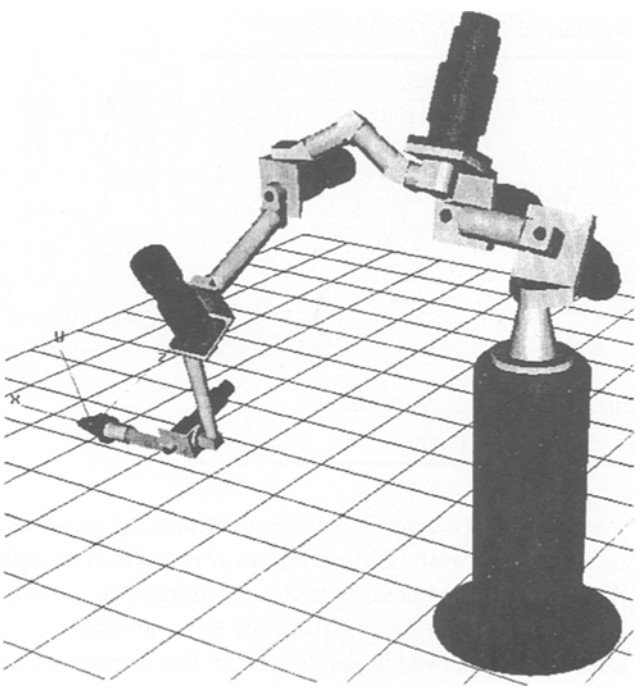

Fig. 6. REDIESTRO at the zero configuration.

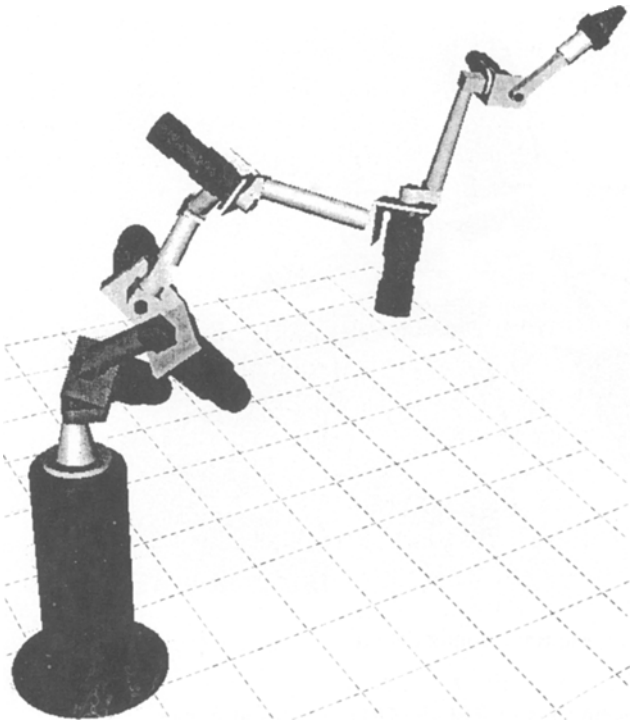

Fig. 7. REDIESTRO at the fully stretched configuration.

As the design of the manipulator was finalized, the detailed CAD drawings of the components were made with the use of AuToCAD™. Furthermore, the solid modeling capabilities of AuToCAD™ were utilized to obtain the inertial parameters of each link, defined in its local coordinate frame. By completing the detailed drawings for each link, a three-dimensional solid model of the corresponding link-actuator sub-assembly was made, and the parameters were estimated. Table VI contains the inertial parameters of the links, namely, the mass, mass-center location and moments and products of inertia. Moreover, a photograph of REDIESTRO in its isotropic configuration is shown in Figure 8.

6. Heuristic Design Rules

In this section, the heuristic design rules that were developed during the course of this design are briefly outlined. To date, most robotic manipulators have been designed with conventional orthogonal architectures. By exploring other general architectures, it is possible to design manipulators for particular or general applications, while considering several kinematic, static or functional design issues. It is concluded that the Jacobian matrix can be used effectively to address design considerations such as synthesis of the kinematic chain, numerical con-

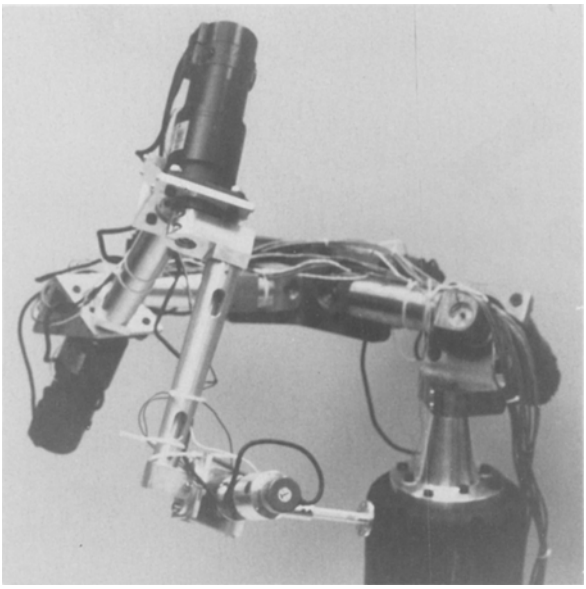

Fig. 8. REDIESTRO at the isotropic configuration.

Table VI. Inertial parameters of REDIESTRO in its local frames

Parameters		link 1	link 2	link 3	link 4	link 5	link 6	link 7
Mass (kg)		17.313	5.580	28.586	7.390	5.987	2.557	0.2
Center of gravity (m)	x	4.8e-4	0.1155	−0.0011	0.3071	0.0	−0.0919	0.06345
	y	−0.1607	−0.0036	−0.1176	−0.1326	0.03434	0.0	
	z	−0.1186	−0.0618	−0.1170	0.0699	−0.3209	0.49	−0.0034
Moments of inertia (kg m^2)	x	0.89926	0.02573	1.6620	0.09297	0.8284	0.6541	0.000024
	y	0.31342	0.13223	0.7860	0.8881	0.7019	0.6714	0.001136
	z	0.62745	0.11099	0.9387	0.8753	0.1317	0.0374	0.001135
Products of inertia (kg m^2)	xy	−2.7e-5	−0.0045	0.0001	−0.1203	0.00009	−0.00839	0.0
	yz	0.3689	0.0012	0.1221	−0.0204	0.26852	0.04574	0.0
	xz	−1.2e-5	−0.0404	0.0003	0.1411	0.00016	−0.12596	0.0

ditioning, singularities of the workspace, extreme reach and workspace volume. Depending on the characteristics of the manipulator and tasks to be performed, priority can be placed on fulfilling one or more of the foregoing demands. For the design of REDIESTRO, we are mainly concerned with the accuracy of the kinetostatic transformations. In this regard, we aimed at the design of an isotropic seven-revolute manipulator. Thus, the highest design priority was given to the realization of an isotropic Jacobian matrix. Other design considerations such

as structural requirements, collision and functionality of the link-actuator sub-assemblies, workspace, extreme reach of the manipulator, and constructability of the links are variables that were prioritized and satisfied accordingly. For instance, the second-priority task for the design of REDIESTRO was concerned with structural considerations, namely, concentration of the first four joints near the base to minimize the static and inertial loads sensed by the proximal drives. It was concluded that pre-determined lower and higher bounds had to be placed on the distance between the second and third axes, i.e., on a_2, in order to best enclose the four proximal drive units, while keeping them in close proximity. The location of each actuator along the corresponding joint axis was determined from the considerations below:

- Minimization of the moment arm created with respect to the previous drive.

When two consecutive joint axes are non-parallel and non-intersecting, the static (dynamic) load sensed by the first drive is affected by the moment arm (radii of gyration), which is in turn affected by the location of the second actuator along its joint axis.

- Creation of collision-free regions around the isotropic configuration.

In order to exploit the inherent well-conditioning characteristics of an isotropic manipulator, or to make use of the large singularity-free regions around the isotropic configurations, it is essential to maximize the accessibility of the corresponding region from a structural view point as well. This can be achieved by minimizing the presence of link segments within the region, and by maximizing the accessible positive and negative range of motion for each joint about its corresponding isotropic point.

- Functionality and constructability of the design.

Focusing strictly on the two previous items can result in link shapes and geometries that are not feasible in terms of manufacturing processes and functionality. Hence, in conjunction with the above-mentioned design issues, one has to take into consideration the constructability by making reasonable compromises against other critical aspects.

It is planned to incorporate the foregoing heuristic rules into an expert system to serve as an aid for the design of advanced manipulator systems. Applications of these systems are anticipated in space and underwater environments.

Acknowledgements

We wish to acknowledge the valuable assistance of Mr. F. Bubic, who produced the preliminary mechanical design. Furthermore, Mr. J. Darcovich, who devel-

oped RVS and customized it for our design applications, is given due acknowledgement. The skillful manufacturing work of Messrs. A. Clément and F. Picard of the Department of Mechanical Engineering at McGill University and of Mr. Serge Lemir, of the counterpart department at Ecole Polytechnique de Montréal, is highly commended. The interfacing of REDIESTRO to its host computer was done very professionally by Mr. K. T. Shafik, our electronics engineer.

The research work reported here was made possible under NSERC (Natural Sciences and Engineering Research Council, of Canada) Grants A4532, STRGP 205, and EQP00-92729. Support from IRIS, the Institute for Robotics and Intelligent Systems, a network of Canadian centres of excellence, is also acknowledged. Mr. González–Palacios was funded partly by Consejo Nacional de Ciencia y Tecnología (National Council of Science and Technology), of Mexico.

References

1. Pieper, D. L: The kinematics of manipulators under computer control, PhD Thesis, Stanford University, CA, 1968.
2. Mavroidis, C. and Roth, B.: Structural parameters which reduce the number of manipulator configurations, in *ASME Biennial Mechanisms Conference*, 13–16 Sept., 1992, Vol. 45, 1992, pp. 359–366.
3. Hayati, S.: Improving the absolute positioning accuracy of robot manipulators, *J. Robotic Systems* **2** (1985), 397–413.
4. Bennett, D. J., Hollerbach, J. M. and Henri, P. D.: Kinematic calibration by direct estimation of the Jacobian matrix, in *Proc. 1992 IEEE Int. Conf. Robotics Automat.* **1** (1992), pp. 351–357.
5. Hollerbach, J. M.: Optimum kinematic design for a seven degree of freedom manipulator, in H. Hanafusa and H. Inoue (eds), *Robotics Research, 2nd Int. Symp.*, MIT Press, Cambridge, MA, 1985, pp. 215–222.
6. Kim, J.-O. and Khosla, P. K.: Framework for task based design of manipulators, in *4th Int. Symp. Robotics and Manufacturing (ISRAM'92)*, Vol. 4, 1992, pp. 27–32.
7. Kim, J.-O. and Khosla, P. K.: A multi-population genetic algorithm and its application to design of manipulators, *IEEE/RSJ Int. Workshop on Intelligent Robots and Systems (IROS'92)*, 1992.
8. Kim, J.-O. and Khosla, P. K.: Task based synthesis of optimal manipulator configurations, *1992 Japan–USA Symposium on Flexible Automation, A Pacific Rim Conference, ISCIE*, San Francisco, CA, 1992.
9. Shmitz, D. E., Khosla, P. K. and Kanade, T.: The CMU reconfigurable modular manipulator system, *Proc. 18th ISIR*, Australia, 1988.
10. Hartenberg, R. S. and Denavit, J.: *Kinematic Synthesis of Linkages*, McGraw-Hill, New York, 1964.
11. Angeles, J., Ranjbaran, F. and Patel, R. V.: On the design of the kinematic structure of seven-axes redundant manipulators for maximum conditioning, in *Proc. IEEE Int. Conf. Robotics Automat.*, Vol. 1, 1992, pp. 494–499.
12. Yoshikawa, T.: Analysis and control of robot manipulators with redundancy, Preprints *1st Int. Symp. Robotics Res.*, Aug. 28–Sept. 2, 1983, Bretton Woods, NH, 1983.
13. Yoshikawa, T.: Manipulability of robotic mechanisms, *Int. J. Robotics Res.* **4** (1985), 3–9.

14. Angeles, J. and López-Cajún, C. S.: Kinematic isotropy and the conditioning index of serial robotic manipulators, *Int. J. Robotics Res.* **11**(6) (1992), 560–571.
15. Klein, C. A. and Blaho, B. E.: Dexterity measures for the design and control of kinematically redundant manipulators, *Int. J. Robotics Res.* **6** (1987), 72–83.
16. Klein, C. A. and Miklos, T. A.: Spatial robotic isotropy, *Int. J. Robotics Res.* **10**(4) (1991), 426–437.
17. Hsu, M. S. and Kohli, D.: Boundary surfaces and accessibility regions for regional structures of manipulators, *Mechanism and Machine Theory* **22**(3) (1987), 277–289.
18. González–Palacios, M. A., Angeles, J. and Ranjbaran, F.: The kinematic synthesis of serial manipulators with a prescribed Jacobian, *1993 IEEE Int. Conf. Robotics Automation*, Atlanta, GA.
19. Whitney, D. E.: The mathematics of coordinated control of prosthetic arms and manipulators, *ASME J. Dynam. Syst., Meas., Contr.* **94**(14) (1972), 303–309.
20. Hunt, K. H.: *Kinematic Geometry of Mechanisms*, Clarendon Press, Oxford, 1978.
21. Golub, G. H. and Van Loan, C. F.: *Matrix Computations*, Johns Hopkins University Press, Baltimore, 1983.
22. Li, Z.: Geometrical considerations of robot kinematics, *Int. J. Robotics Automation* **5**(3) (1990), 139–145.
23. Salisbury, J. K. and Craig, J. J.: Articulated hands: Force and kinematics issues, *Int. J. Robotics Res.* **1** (1982), 4–17.
24. Angeles, J.: The design of isotropic manipulator architectures in the presence of redundancies, *Int. J. Robotics Res.* **11**(3) (1992), 196–201.
25. Angeles, J., Pfeiffer, F. and Weidemann, H.-J.: The kinematic design of walking machines under isotropy criteria, *3rd Int. Workshop on Advances in Robot Kinematics*, *Ferrara*, 7–9 Sept., 1992, pp. 230–235.
26. Saha, S. K., Angeles, J. and Darcovich, J.: The kinematic design of a 3-dof isotropic mobile robot, *1993 IEEE Int. Conf. Robotics and Automation*, Atlanta, GA, 1993.
27. Kim, J.-O. and Khosla, P. K.: Dexterity measures for design and control of manipulators, in *IEEE/RSJ Int. Worshop on Intelligent Robots and Systems* (IROS'91), 1991, pp. 758–763.